Procedia Computer Science

Volume 29, 2014, Pages 855–865

ICCS 2014. 14th International Conference on Computational Science

A physics-based Monte Carlo earthquake disaster simulation accounting for uncertainty in building structure parameters

Shunsuke Homma[1], Kohei Fujita[1], Tsuyoshi Ichimura[1], Muneo Hori[1], Seckin Citak[2], and Takane Hori[2]

[1] University of Tokyo, Japan
{homma,fujita,ichimura,hori}@eri.u-tokyo.ac.jp
[2] Japan Agency for Marine-Earth Science and Technology, Japan
{citak,horit}@jamstec.go.jp

Abstract

Physics-based earthquake disaster simulations are expected to contribute to high-precision earthquake disaster prediction; however, such models are computationally expensive and the results typically contain significant uncertainties. Here we describe Monte Carlo simulations where 10,000 calculations were carried out with stochastically varied building structure parameters to model 3,038 buildings. We obtain the spatial distribution of the damage caused for each set of parameters, and analyze these data statistically to predict the extent of damage to buildings.

Keywords: earthquake disaster simulation, Monte Carlo simulation, high performance computing

1 Introduction

An earthquake may lead to widespread disaster, and is a serious risk for large urban areas. At present, statistical methods such as fragility curves are typically used for earthquake disaster prediction. Fragility curves are empirical relations describing building structure damage as a function of earthquake intensity. However, these methods are based on historical data, so generally are not sufficient to describe the specific characteristics of earthquakes and building structures. To create a high-precision and high-resolution earthquake disaster prediction model, we are developing a system called the Integrated Earthquake Simulator (IES) [1], which implements large-scale earthquake simulations and integrates reliable physics-based analysis methods and geographic information system (GIS) data. This high-precision and high-resolution disaster simulation method is expected to help create disaster mitigation policies, efficient risk-shifting, and rapid evacuation and recovery.

Selection and peer-review under responsibility of the Scientific Programme Committee of ICCS 2014

doi:10.1016/j.procs.2014.05.077

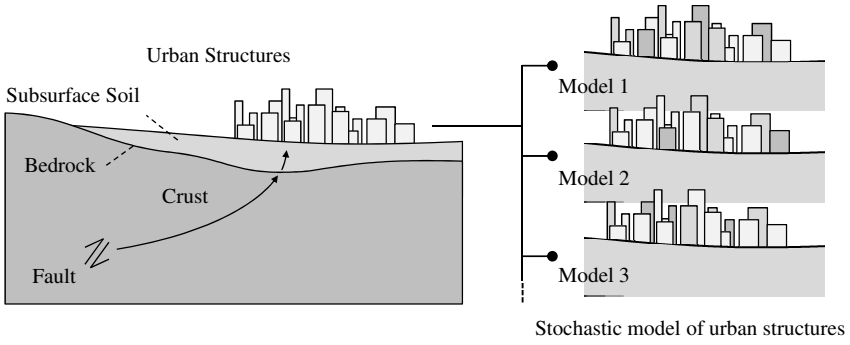

Figure 1: An illustration of the Monte Carlo method for earthquake simulation. The left panel shows a cross-section, illustrating the fault-to-city system of fault rupture, wave propagation in the crust, soil amplification, and structure response. The earthquake ground motion of the bedrock is estimated using a Stochastic Green's Function (SGF) simulation technique, which considers fault rupture and wave propagation in the crust. The response of the city is computed through the physics-based soil amplification and seismic structural response analysis. The right panel illustrates the stochastic building structures model, where uncertainty in the parameters is accounted for by running multiple simulations with stochastically varied input parameters, material's elasticity and strength.

High-performance computing (HPC) is required for IES[2], because physics-based simulation of an entire city is a computationally expensive task. HPC allows IES to use high-resolution models of soil and building structures, and with IES, we can model an entire city in considerable detail using GIS data. We also require HPC for the multiple cases that are included in the Monte Carlo simulation (MCS), i.e., to model numerous possible earthquake scenarios. IES can model 1,000 earthquake scenarios for 253,405 buildings in Tokyo in 3,446 s; however, this requires the use of 20,000 nodes of the K-computer, which is the largest supercomputer in Japan, and the existing implementation of IES does not consider uncertainty in the model of the building structures.

In this study, we address uncertainty in the physics-based simulation model. In earthquake simulation, the models of faults, the crust, soil, and building structures typically contain significant uncertainties that originate from non-uniformity of material and incomplete survey data. MCS is an approach for managing uncertain parameters, by including a probability distribution of those parameters. Here we use IES with a Monte Carlo method to account for uncertainties in building structure parameters. Figure 1 shows an overview of the simulation process. We simulated 10,000 parameter sets describing an earthquake disaster event in Onagawa, Japan, which has 3,038 building structures. We obtain the stochastic variation in the spatial distribution of damage to building structures.

2 Simulation Method

Currently, a range of simulation methods are used in the fields of earthquake engineering and Earth science. We may also utilize GIS data, which are typically very detailed in urban areas.

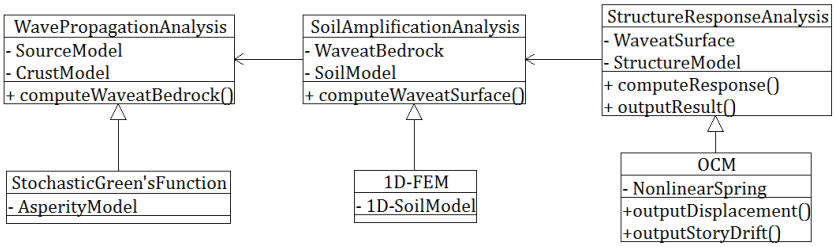

Figure 2: An illustration of the simulation process.

In this study, we used IES, which integrates several simulation methods and data conversion methods. For high-precision and high-resolution earthquake disaster prediction, we should consider the entire response of the system, i.e., fault rupture, wave propagation in the crust, soil amplification, and the response of the building structures. IES produces a seamless "fault-to-city" simulation that can describe the whole process of an earthquake, and the resulting damage to buildings. In addition, the spatial distribution of damage over a large area can be used to make evacuation and recovery plans. In the following section, the IES simulation method is described, and in the subsequent sections, methods to simulate and model aspects of earthquake disaster simulation are detailed.

2.1 IES

There are three modules in the simulation: wave propagation analysis (WPA), soil amplification analysis (SAA), and structure response analysis (SRA). Figure 2 shows an outline of the simulation process. The reference relationship of the analysis modules, their functions, and their input models are shown. The WPA module includes the generation of an earthquake wave at a fault and subsequent propagation through the crust. The SAA module computes the amplification of the earthquake wave as it propagates through the soft subsurface soil. The SRA module describes the effects of the earthquake wave at the surface. The flow of the simulation is unidirectional, so that each module takes input data only from the module of the previous step.

2.2 Modules

The analysis methods used for each module are also shown in Figure 2. We use Green's functions[3] for the WPA module. Green's functions are used to compute the earthquake wave in the bedrock, using historical earthquake records and general characteristics of the Fourier spectrum of the earthquake. The fault and crust models employ data including the velocity-structure dispersion relation of the crust, which can be investigated experimentally using methods including deep-layer boring [4]. Results of WPA changes according to the position, therefore WPA is carried out several times when the target area is huge. For the SAA module, we use a one-dimensional finite element method (1D FEM) to model the wave propagation through nonlinear soil. The soil model was constructed based on boring data surveyed by government and construction companies. Spatial interpolation was used to obtain the 3D soil structure, using discrete boring data[5]. SAAs' results sensitively changes according to each soil structure of the position rather than WPA, therefore SAA is carried out for all target structures respectively.

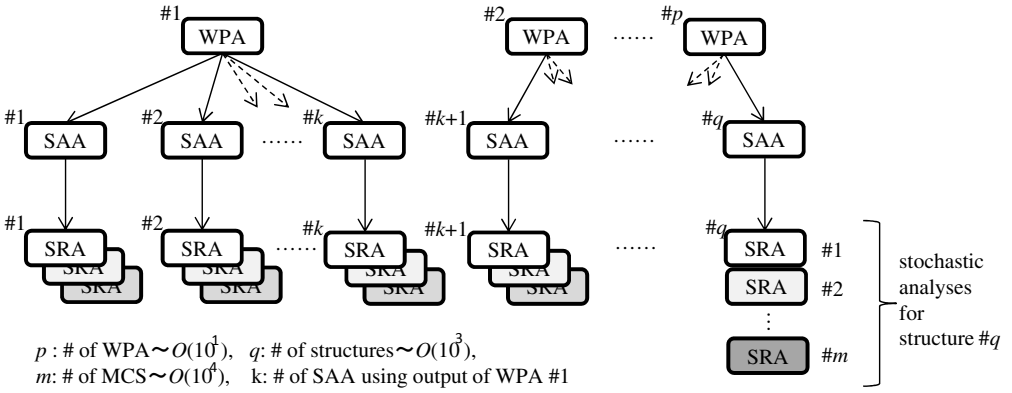

Figure 3: The flow of data within the MCS.

For the SRA module, we used a one component model (OCM), which is a frame model, where beams and columns are modeled as combinations of nonlinear springs. The structures model was constructed using GIS/CAD data[5] on only the position and shape of structures. We can utilize a procedure for structure design to estimate a reliable structures model with only limited information. Using these techniques, the earthquake wave is treated as time-series data, which allows the SAA and SRA modules to carry out a nonlinear analysis.

2.3 Application of HPC

The number of implementations of each module in the MCS and the way of parallelization are described in this section.

The flow of data between modules in the Monte Carlo earthquake disaster simulation is shown in Figure 3. The result of WPA#1 is browsed by SAA#1-#k that carried out directly under SRA#1-#k. WPA is carried out p times for divided p areas on the bedrock. m is the number of stochastic models for each structure, namely the number of MCS. The SRA module incurs the largest computational cost (of order $10^7 = q * m$) to make the MCS of each structure in the target area. Considerable computational cost is also incurred in the SAA module (of order $10^3 = q$), as this module models the wave at the surface under each structure. The computational cost for the WPA module is the lowest, because only a few points (of order of $10^1 = p$) are calculated per city. Thus, we apply HPC methods to the SAA and SRA modules only. We developed a parallel implementation, whereby the SAA and SRA modules are separate processes, and wave data at the surface are passed between these modules via the file system. The SAA and SRA modules were implemented in a procedural manner to analyze one soil column or structure at a time. To compute many points and structures in a city, we parallelized this calculation by distributing the soil columns and structures as separate processes of a distributed computer, and executed these analyses in parallel. For the SAA module, we use an all-worker model, with static load-balancing at the start of the simulation using the measured runtime of a short input wave. This load-balancing is effective because the runtime for each time step is similar regardless of the amplitude of the input wave.

Quotas of structures for processes in the MCS is shown in Figure 4. We group processes into the m cases, each with the same number of processes, n, and each group carries out an analysis

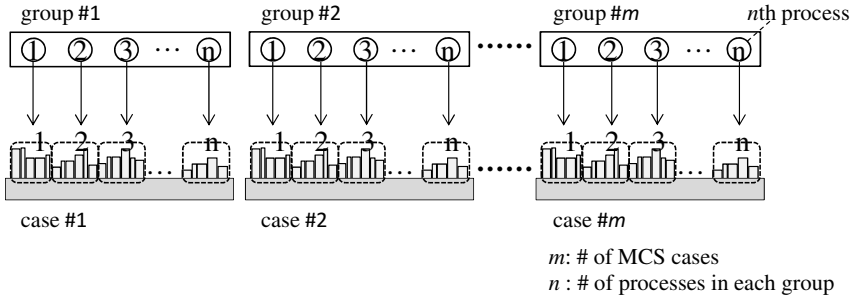

Figure 4: The distribution of structures in terms of computational processes.

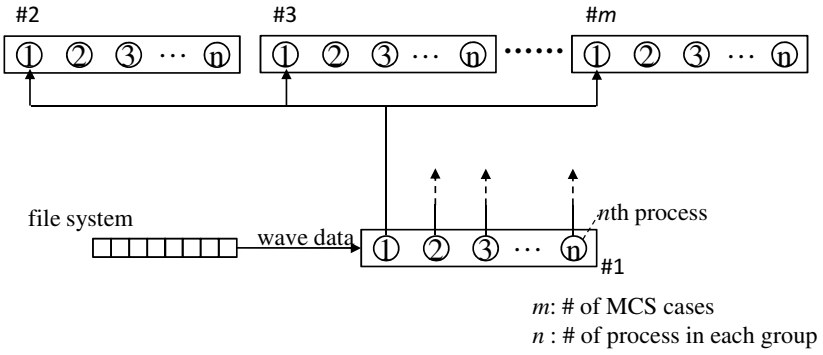

Figure 5: The data distribution between processes for SAA.

using different structural parameters. Load-balancing was carried out within each group using the same method as that used in the SAA module.

File input/output (I/O) optimization is required for scalability, as considerable I/O is required to pass the time history data between modules. Outputting data for each point/structure to individual files leads to a large number of small files. Hence, we grouped the results of points/structures to reduce the number of files and improved the I/O throughput. Figure 5 shows the data distribution for MCS using the SRA module. For the SAA module, the wave computed at the surface by all processes is collated and outputted to a single file, using a collective write function of MPI-IO (i.e., MPI_File_write_at_all()). Processes in group #1 read wave data at the surface using a collective read function (i.e., MPI_File_read_all()), and broadcast the input waves to all processes in the other groups. The maximum response of each case is outputted to the file system by collecting the output and sending it to the root process of each case, and outputting the results to the shared file system using serial output (MPI_File_write()).

3 Application

3.1 Performance Measurement

Here, we measure the parallel performance of IES. In the SRA module, 1 node (8 processes) of the K-computer calculates 2 cases of the simulation, i.e., 4 processes are used per case. We obtained the ground motion data at the position of each of the building structures using the deterministic SAA model, so that multiple calculations were carried out using the SRA module for each dataset. The size of each input dataset describing the ground motion was 867 MB; there were 3,038 building structures, and the number of time steps in the analysis was 25,000; this leads to 50,000 output files with a total size of 25 GB, when analyzing 10,000 cases.

The computational time for simulations of 2 cases and 10,000 cases are listed in Table 1. The problem is first initialized, which includes reading the configuration file, static load-balancing, and converting the structure data. Following this, the input includes reading and broadcasting the earthquake wave data to each structure of the many-case analysis (see Figure 5). The analysis includes running the SRA module. During output, the maximum displacement and story drift angles are written to a file. The vast majority of the time for computation was incurred by the SRA module, which shows that the file I/O is not a significant part of the computational cost of the simulation. We can check the weak scalability, i.e., how the simulation time changes with the number of cases, where the number of processes used to analyze each case is fixed. Comparing the time for computation between the 10,000-case simulation and 2-case simulation, the weak scaling is more than 97.5%. Therefore, we may conclude that parallelization of the many-case simulation was effective.

	initialization	input of ground motion	analysis	output	total
2-cases (1 node)					
Max	17.10	8.11	19668.51	7.30	19701.0
Min	17.09	7.99	19621.99	0.00	19693.7
Average	17.10	8.05	19647.64	4.51	19698.2
10,000-cases (5,000 nodes)					
Max	116.80	22.33	19708.61	352.80	20199.1
Min	114.86	18.02	19587.40	0.00	19846.3
Average	116.14	21.22	19647.02	88.36	19934.7

Table 1: The time for computation for each process in seconds.

3.2 Deterministic Simulation

First, we discuss a single-case deterministic simulation in Onagawa, Tohoku, Japan, which had 3038 structures and was severely damaged by the Tohoku Earthquake and Tsunami in 2011. We used the fault model of the Tohoku Earthquake proposed by Kurahashi and Irikura[6] for the Stochastic Green's Function (SGF) simulation. The 1D FEM soil model was constructed using geologic cross-section data, as well as data on the deep layer structure[7], as shown in Figure 6. We used a B-spline to interpolate between soil layers, and we used GIS data from NTT-GEOSPACE[8] to construct the structure model of the OCM. The duration of earthquake was approximately 250 s, and the number of time steps was set to 25,000, at 0.01 s intervals.

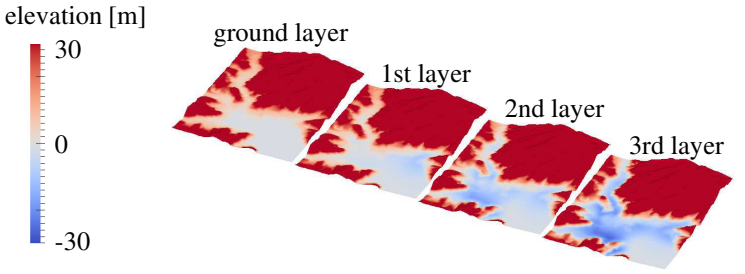

Figure 6: The ground elevation and boundary surfaces of the soil.

The target area does not contain an available observation point, and so we choose the nearest observation point[9] in Ishinomaki and to compare the results of our simulation with the measured data. A comparison of calculated and observed velocity waves at the surface is shown in Figure 7. In the north-south (NS) direction, the phase was consistent, although the amplitude of the calculated wave was smaller than the observed data. In the east-west (EW) direction, we can see four features in both the measured and simulated data; however, the amplitude was smaller in the simulation. We may improve the precision using, for example, 3D FEM[10] for the WPA module; however, this is very computationally expensive, and therefore the high-frequency component of the earthquake should be calculated using a SGF and the low-frequency component using 3D FEM. Improving the precision of the earthquake wave model has been identified as an area for further development.

Figure 8 shows the maximum story drift angles of each structure, their spatial distribution, and the elevation of the surface. We can use the maximum story drift angle as an index of the damage to each structure. If the maximum story drift angle is larger than 0.02°, we may expect serious damage to occur. The simulated response was large around the coastal area, which is due to the thickness of subsurface soil: compared to the results shown in Figure 6, we can see that the subsurface soil was thicker in this large response area. It is generally expected that the thicker the soft subsurface soil is, the stronger the earthquake will be.

3.3 Stochastic Simulation

We construct all structure models assuming reinforced concrete (RC) structures, and focus on the uncertainty in the parameters describing concrete. Concrete has wider variation in performance than most other building materials. We estimated the probability distributions of the elasticity and strength of concrete, together with the correlation between the two, based on the open database[11]. We assume that both the elasticity and strength can be described by a normal distribution for simple application. Figure 9 shows the probability density function (PDF) and the survey data. If the given value excesses the $\mu \pm 2\sigma$ or $\mu \pm 3\sigma$ (μ and σ are the mean and standard deviation values of the PDF), we try to get the value again in order to avoid getting negative values. In this simulation, the number of cases was $m = 10,000$ and the number of processes in each group was $n = 4$ (see Figure 5).

3.3.1 One stochastic parameter

Here we treat only elasticity as a stochastic parameter. The time for computation of these simulations was 20,199 s (5.6 h), and 40,000 processes were run on 5,000 nodes of the K-computer.

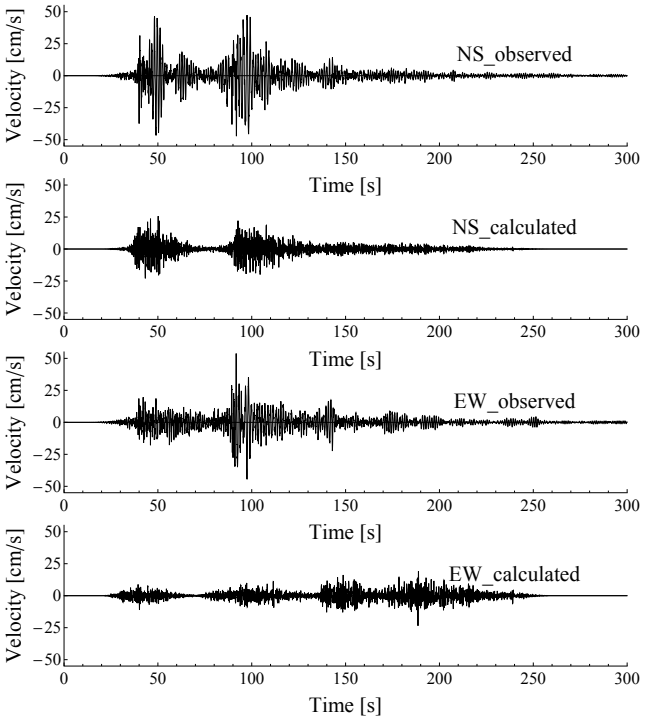

Figure 7: The observed and calculated surface velocity at the Ishinomaki observation point.

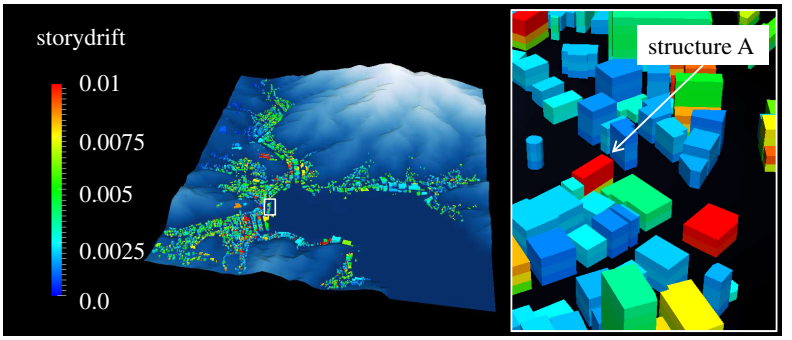

Figure 8: The spatial distribution of building damage using the deterministic simulation, showing the maximum story drift angles of structures in Onagawa. The position of structure A is also illustrated.

Figure 10 shows the spatial distribution of the maximum story drift angle for all 10,000 cases, together with the mean and standard deviation of these data. The spatial distribution of the mean story drift angle showed a stronger correlation with the maximum values than with the standard deviation. It follows that the response of structures depends mainly on the input earthquake wave; however, we also need to consider the levels of earthquake resistance of the structures. Consider structure A, a three-story building shown in Figure 8. Figure 11 shows

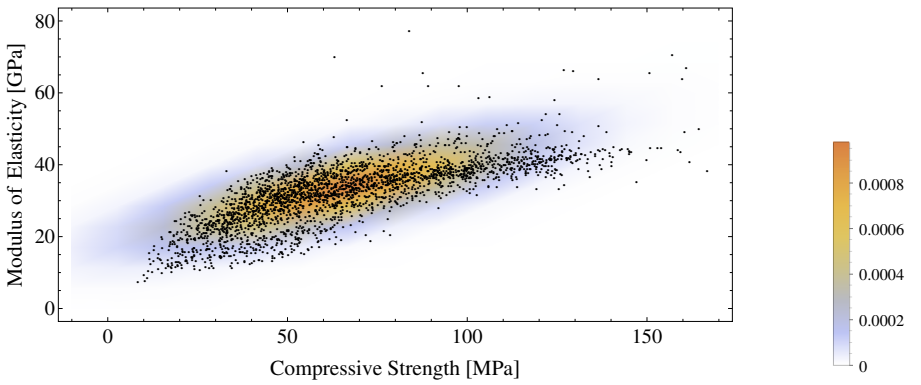

Figure 9: The survey data of the mechanical properties of concrete (black dots[11]) and the two-dimensional fitted normal distribution in color scale.

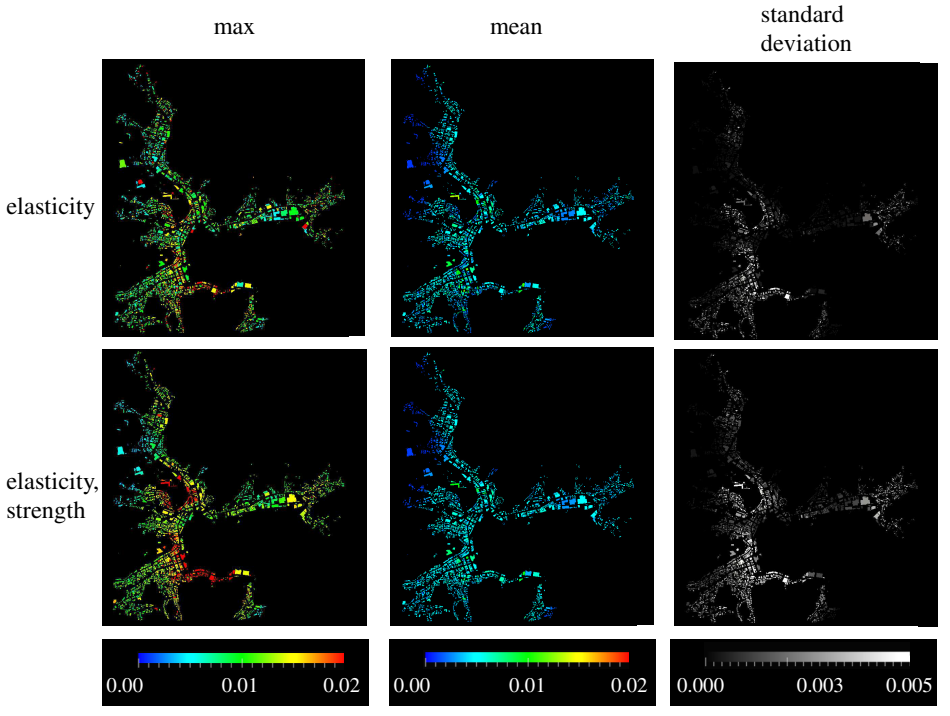

Figure 10: The maximum, mean, and standard deviation of the story drift angles. The top row shows data for the stochastically varied elasticity, and the bottom row shows data for stochastically varied elasticity and strength.

histograms of the number of times that structure A exhibited a given maximum story drift angle. These data are bimodal, which can be explained by considering that, once the response of a structure becomes large, we may expect nonlinear behavior, which leads to a large response once a threshold has been reached.

stochastic parameter: elasticity

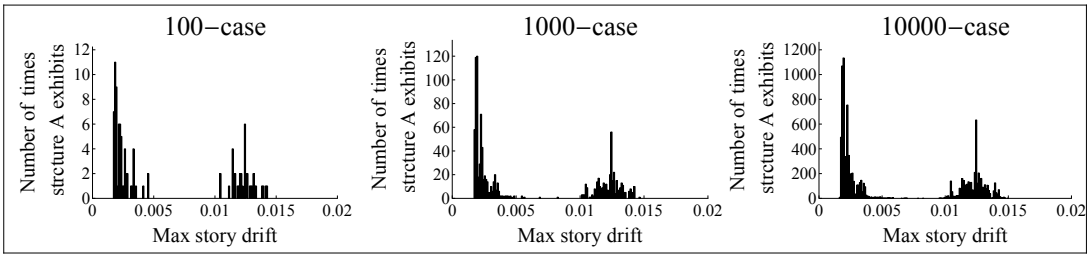

stochastic parameter: elasticity, strength

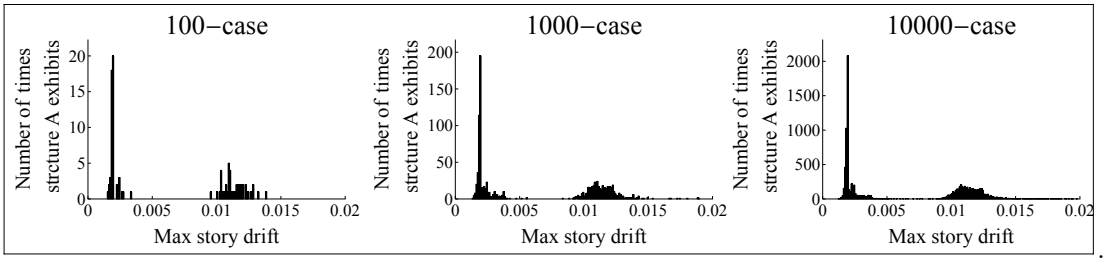

Figure 11: Histograms showing the maximum story drift angle of structure A for simulations with one and two stochastic parameter.

3.3.2 Two stochastic parameters

Here we consider strength as a stochastic parameter in addition to elasticity. The time for computation here was 20,208 s (5.6 h), with 40,000 processes running on 5,000 nodes of the K-computer. Again, we obtained the maximum story drift angles for each structure, together with the mean and standard deviation, as shown in Figure 10. The maximum and the standard deviation of the data were larger than with only one stochastic parameter; however, the mean values did not change significantly. Consider structure A again; the histograms shown in Figure 11 also converge to a bimodal distribution. The peak corresponding to small drift angles was very sharp, and the second peak was broader than for the case when only one stochastic parameter was used. In this case, histograms seem converged enough with 10,000 MCS. And we can see that with the increase of the number of uncertain values, the needed number of MCS for convergence increased. It is expected that the number of uncertain values in soil and earthquake fault are larger than that of structures. In the future research, we would like to discuss the utilization of these results for prevention or reduction of disaster, and quantitatively show the necessary number of MCS.

4 Conclusion

We have described an MCS approach for physics-based earthquake disaster simulations, which accounts for uncertainty in the input parameters of the building structures model. We created a stochastic structures model and examined the influence of the uncertainties in the parameters on the maximum story drift angle. We obtained a spatial distribution of damage to structures. This high-precision and high-resolution earthquake disaster simulation is expected to be useful for evaluating disaster mitigation policies and implementing efficient risk assessment by insurance or finance companies. We would like to study the utilization of these results and how to quantitatively show the reliability of earthquake disaster estimation. Furthermore, we need to tackle the problem of uncertainty of ground motion which has larger uncertainty than structures.

Acknowledgments The geological cross-section data for Onagawa were provided by Mr. Nakatani, who leads the urban planning section of the Onagawa office, and Dr. Sugawara from Tohoku University acted as an intermediary for this. The authors would like to thank both for their valuable input. Much of the data presented here were obtained using the K computer at the RIKEN Advanced Institute for Computational Science, Japan.

References

[1] M. Hori and T. Ichimura. Current State of Integrated Earthquake Simulation for Earthquake Hazard and Disaster. *Journal of Seismology*, 12(2):307–321, 2008.

[2] M. L. L. Wijerathne, M. Hori, T. Kabeyazawa, and T. Ichimura. Strengthening of Parallel Computation Performance of Integrated Earthquake Simulation. *Journal of Computing Civil Engineering*, 27(5):570–573, 2013.

[3] D. M. Boore. Stochastic Simulation of High-Frequency Ground Motions Based on Seismological Models of The Radiated Spectra. *Bulletin of the Seismological Society of America*, 73(6):1865–1894, 1983.

[4] H. Fujiwara, M. Ooi, and S. Kawai. Development of An Integrated Geophysical and Geological Information Database for Strong-Motion Evaluation. *The 14th World Conference on Earthquake Engineering*, 2008.

[5] F. Yang, T. Ichimura, and M. Hori. Earthquake Simulation in Virtual Metropolis Using Strong Motion Simulator and Geographic Information System. *Journal of Applied Mechanics*, 5:527–534, 2002.

[6] S. Kurahashi and K. Irikura. Source Model for Generating Strong Ground Motions During The 2011 Off The Pacific Coast of Tohoku Earthquake. *Earth, Planets and Space*, 63(7):571–576, 2011.

[7] National Research Institute for Earth Science and Disaster Prevention. Japan Seismic Hazard Information Station. `http://www.j-shis.bosai.go.jp/en/`.

[8] NTT GEOSPACE. `http://www.ntt-geospace.co.jp/`.

[9] National Research Institute for Earth Science and Disaster Prevention. Strong-motion seismograph networks (k-net,kik-net). `http://www.kyoshin.bosai.go.jp/`.

[10] T. Ichimura, M. Hori, P. E. Quinay, M. L. L. Wijerathne, and T. Suzuki. Comprehensive Numerical Analysis of Fault-structure Systems - Computation of The Large-scale Seismic Structural Response to A Given Earthquake Scenario -. *Earthquake Engineering and Structural Dynamics*, 41(4):795–811, 2012.

[11] Noguchi, T. Database for Mechanical Properties of Concrete. `http://bme.t.u-tokyo.ac.jp/researches/detail/concreteDB/index.html`.